Low voltage ride-through capability of distributed generator connected to the grid through the back-to-back converter

Zoran Ivanović, Evgenije Adžić, Stevan Grabić, Vlado Porobić, Vladimir Katić

University of Novi Sad
Faculty of Technical Sciences
Novi Sad, Serbia
zorani@uns.ac.rs, evgenije@uns.ac.rs, grabics@uns.ac.rs, poroba@uns.ac.rs, katav@uns.ac.rs

Abstract—**This paper deals with low voltage ride-through capability of distributed generator unit. Distributed generator, considered in this paper, is based on squirrel cage induction machine and it is connected to the grid through the back-to-back converter and LCL filter. With an increasing distributed generation grid connection requirements in almost every country require generation unit to stay connected to the grid and ensure active and reactive power injection. In this paper we proposed improved dual vector current controller to deal with the unbalance imposed by the electrical grid. Controller provides injection of active and reactive power to the grid, even if the voltages are lower than the nominal one. Results are validated using contemporary hardware-in-the-loop emulation platform, while controller is based on TMS320F2812 DSP.**

Keywords-distributed generation; voltage ride-through capability, back-to-back converter; hardware-in-the-loop.

I. INTRODUCTION

Distributed generation (DG) play very important role as a means of achieving increased power system reliability [1]. Wind energy systems, photovoltaic and small hydro plants are commonly employed type of DG units. They have a lot of positive impacts on the grid such as, lower capital costs due to smaller size and possibility to contribute to the overall system stability. Most of distributed generation use renewable sources and they require a lot of power electronics interface to match DG characteristic with the grid requirements [2], [3]. Controllable power electronics interface is most often realized in the form of voltage source convertor (VSC). One complete DG system is shown in Fig. 1. Squirrel cage induction generator is connected through the back-to-back converter, LCL filter and transformer to the grid.

In the past there was no requirement by the grid code for a DG to stay connected to the grid during the fault or grid disturbances [4]. The main focus was on protection of DG unit itself. In the last decade, increasing DG penetration, especially wind energy systems lead to fast establishment of variety of grid codes, which define behavior of DG unit in unconventional conditions. Grid code requirements vary from country to country. One of the most commonly used is adopted by the company E.ON Netz. According to this grid code

requirements it is defined that in the event of faults in the grid, the generating plants must stay connected and inject active and reactive power. These grid code requirements are illustrated in the Fig. 2. It shows the limit curve for the voltage pattern at the grid connection of induction generator based generating plant.
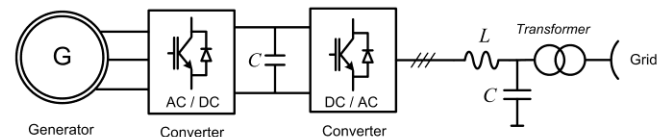

Figure 1.   Figure 2 DG unit connected to the grid through the power electronic interface
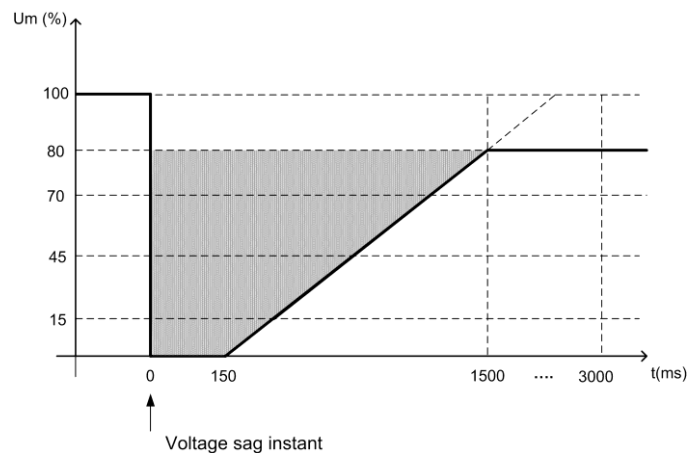

Figure 2.   Figure 1 E.ON grid requirements for DG connection

There are many grid codes which require grid support by active and reactive power injection during the fault in the event of voltage sags. However, specific requirements depend on the specific characteristics of each power system and the protection method employed.

In this paper one control algorithm which solves some power quality problems in case of grid voltage sags is presented. Balanced and unbalanced voltage sags are considered. Controller is based on standard dual vector current

control technique and introduces regulation of negative sequence component.

Tests on DG systems is difficult to carry out in real laboratory due to high power rating of the hardware, system complexity, difficulty associated with the generation of desired grid voltage profile, and impartibility to disconnect DG unit form the system. Instead of working on a real system we can use real-time emulator where power stage is emulated on appropriate high speed platform, while controller is real. Here, we used HIL emulation platform to evaluate the ability of proposed control algorithm to meet grid code requirements in severely balanced and unbalanced grid conditions[5], [6]. The entire hardware is emulated in real–time on the FPGA platform with a fixed simulation step time of 1 µs. The FPGA based platform interacts with the controller through the custom made I/O board. The control algorithm is realized using a control platform based on the TMS320F2812 DSP.

II. VOLTAGE SAGS

A three phase fault in the system leads to an equal voltage drop in each phase. Nonsymmetrical faults leads to drops in one, two or three phases, with not all phases having the same drops [7]. Unbalanced voltage sags caused by network faults introduce negative sequence grid voltage and current components. The control and operation of a grid-connected VSC under these circumstances have been widely investigated in the literature [8]–[18].

One example of unbalanced voltage sag is shown in Fig. 3. Voltages in two phases drop down to 50 % of the nominal one, while third phase remain the same. Disturbance lasts for 3 periods.
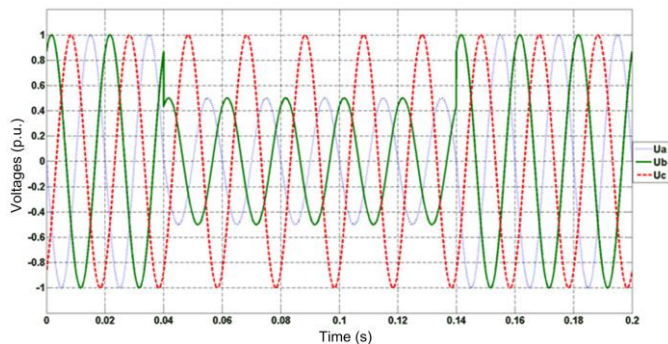

Figure 3.   Unbalanced voltage sag

In order to calculate balanced voltage sag amplitude in the radial distribution networks, we can use the schematic shown in Fig. 4. Z_s represents impedance of the source connected to the point of common coupling (*pcc*), while Z_F represents impedance between *pcc* and place of faults.
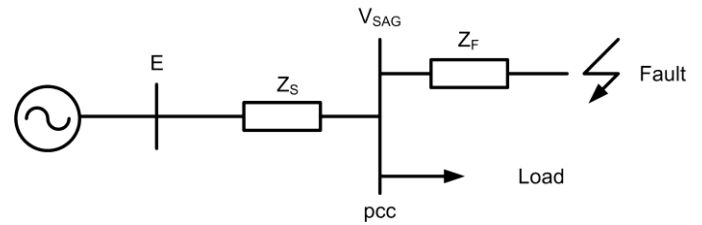

Figure 4.   Unbalanced voltage sag

Remained voltage (voltage at pcc) could be calculated as:

$$V_{sag} = \frac{Z_F}{Z_S + Z_F} \cdot E \qquad (1)$$

If the fault location is closer to the *pcc*, than impedance Z_F will be smaller, so remained voltage will be lower (Z_F has lower value). In case of unbalanced voltages, schematic from Fig. 4 cannot be used. It is necessary to use symmetrical components domain. Equivalent circuit from Fig. 4 should be separated to positive, negative and zero sequence components in order to calculate voltages and currents properly. Detailed analyses of all possibilities are thoroughly explained in [19] and [20]. There are seven basic voltage sag types according to the ABC classification. They are shown in the Figs. 5 and 6.
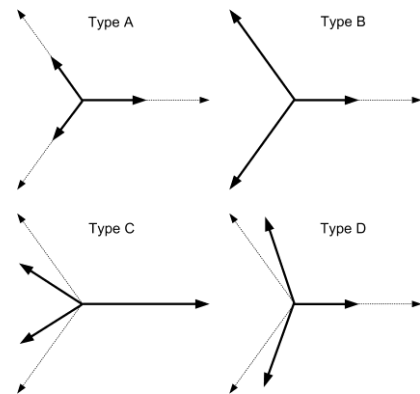

Figure 5.   Voltage sags types – ABC classification (a)
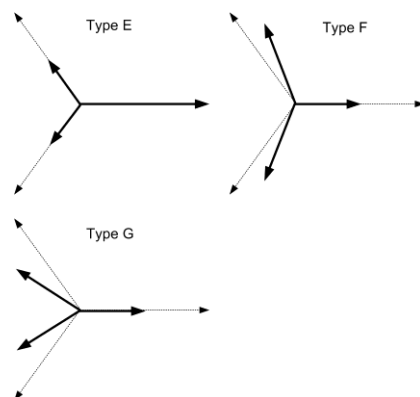

Figure 6.   Voltage sags types – ABC classification (b)

Voltage sags A – D are caused by one-phase, two-phase or three-phase short circuit, while voltage sags E – G are consequence of two-phase to ground short circuit. If there is any transformer in the system, like in Fig. 7 it can lead to changing of voltage types at the converter terminals from one form to another one [7].
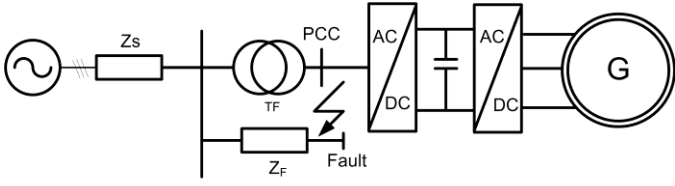

Figure 7. DG unit connected to the grid

Regardless winding connection of the transformer, voltage sag classification mentioned in Figs. 5 and 6 include all possible cases and explain the propagation of three-phase unbalanced sags from one voltage level to another [7].

III. SYSTEM DESCRIPTION UNDER UBALANCED GRID VOLTAGES

In unbalanced systems voltages and currents can be represented by its positive and negative sequence equivalents. A fast and precise detection of both, the positive and the negative sequence angle and magnitude of the voltage component is a vital issue during transient faults in the grid.

Therefore, an unbalanced system of the three phase-voltages (u_a, u_b, u_c) could be represented with its positive ($u_{dq}^p = u_d^p + ju_q^p$) and negative sequence ($u_{dq}^n = u_d^n + ju_q^n$) components, as given by:

$$u_{\alpha\beta} = e^{j\omega t}u_{dq}^p + e^{-j\omega t}u_{dq}^n \qquad (2)$$

where $u_{\alpha\beta} = \sqrt{2/3}\left(u_a + u_b e^{j2\pi/3} + u_c e^{-j2\pi/3}\right)$ is the grid voltage vector expressed in the stationary reference frame (using a power-invariant transformation) and ω is the angular grid-frequency. In the same manner, unbalanced grid-currents also appear and they could be represented in terms of positive and negative sequence current components, similarly to (2):

$$i_{\alpha\beta} = e^{j\omega t}i_{dq}^p + e^{-j\omega t}i_{dq}^n \qquad (3)$$

where ($i_{dq}^p = i_d^p + ji_q^p$) and ($i_{dq}^n = i_d^n + ji_q^n$).

One case of unbalanced grid-voltages in the original and synchronously rotating reference frame is shown in Fig. 8. It should be noted that in the positive sequence reference frame, a positive component appears as DC, whereas a negative component oscillates at twice the grid frequency. In the negative reference frame, it is the opposite, which is explained thoroughly in [12].
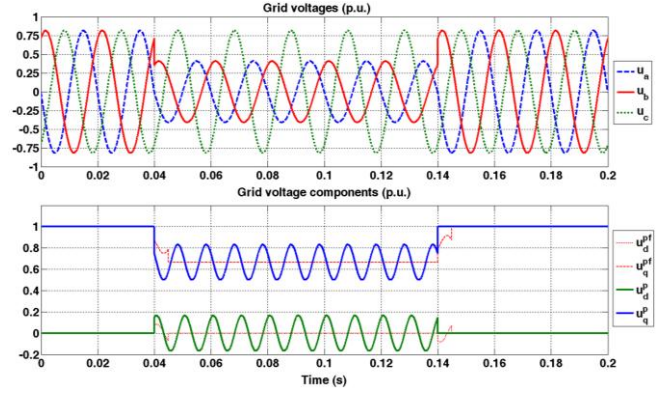

Figure 8. DG unit connected to the grid

The representation of a two-level VSC, used as an actuator in DG application, could be described by differential equation (4) in the stationary reference frame:

$$v_{\alpha\beta} = u_{\alpha\beta} + L\frac{di_{\alpha\beta}}{dt} + Ri_{\alpha\beta} \qquad (4)$$

where R is grid resistance, L is grid inductance and

$$v_{\alpha\beta} = \sqrt{\frac{2}{3}}\left(v_a + v_b e^{j2\pi/3} + v_c e^{-j2\pi/3}\right) \qquad (5)$$

$$i_{\alpha\beta} = \sqrt{\frac{2}{3}}\left(i_a + i_b e^{j2\pi/3} + i_c e^{-j2\pi/3}\right) \qquad (6)$$

where $v_{\alpha\beta}$ and $i_{\alpha\beta}$ denote converter pole voltages and the line currents respectively.

Equation (4) can now be transformed and decomposed into two parts in the positive and negative synchronous rotating reference frames, respectively, as shown in (7) and (8) [12]:

$$v_{dq}^p = L\frac{di_{dq}^p}{dt} + Ri_{dq}^p + j\omega Li_{dq}^p + u_{dq}^p \qquad (7)$$

$$v_{dq}^n = L\frac{di_{dq}^n}{dt} + Ri_{dq}^n - j\omega Li_{dq}^n + u_{dq}^n \qquad (8)$$

With regards to this, instantaneous apparent power could be expressed as:

$$s = u_{\alpha\beta}i_{\alpha\beta}^* = p(t) + jq(t) \qquad (9)$$

where active power $p(t)$ and reactive power $q(t)$ are:

$$p(t) = P_0 + P_{c2}\cos(2\omega t) + P_{s2}\sin(2\omega t) \qquad (10)$$

$$q(t) = Q_0 + Q_{c2}\cos(2\omega t) + Q_{s2}\sin(2\omega t) \qquad (11)$$

Terms P_0 and Q_0 designate the value of the average power, while P_{c2}, P_{s2}, Q_{c2} and Q_{s2} are the magnitudes of the power oscillations caused by the unbalance. Detailed expressions for all six terms are given in [12].

IV. CONTROL ALGORITHM DESCRIPTION

The block scheme of the DG system is represented in Fig. 9. The back to back converter which is fed from squirrel cage induction generator unit is connected to the grid through the LCL filter and grid impedance. Transformer is also used between grid and DG unit. Three phase grid currents and voltages are measured and transformed to dq domain using the transformation angle which is obtained by employing phase look loop (PLL) estimator. Voltages and currents in dq domain are used to calculate active and reactive power according to Equation (10) and (11). These expressions are used in order to design dual vector current controller, which is employed in case of unbalanced voltages.
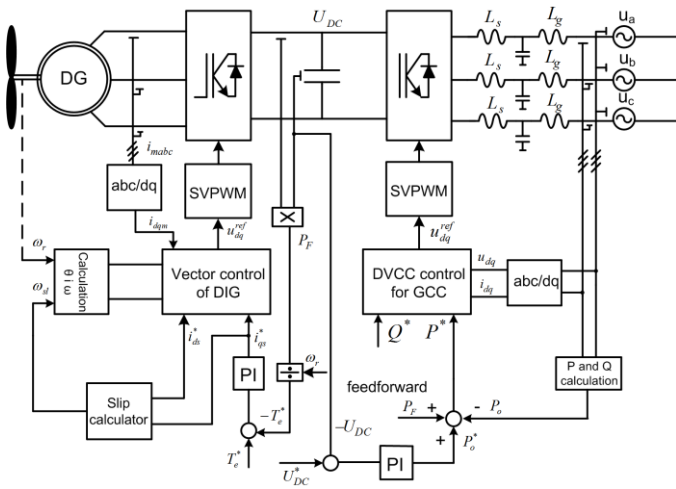
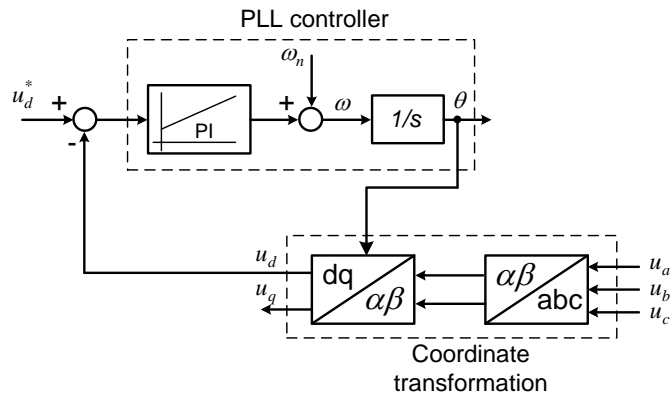Figure 9. DG unit connected to the grid

Figure 10. Determination of grid voltage angle (PLL)

The current controller (DVCC) used here consists of a pair of PI controllers that control the positive and negative sequence components separately and are implemented in two different,

rotating reference frames. Details about the controllers and the extraction of sequence components can be found in [8] and [12]. DVCC controller is shown in Fig. 11.

In order to generate the proper current references, we should consider the following equation:

$$\begin{bmatrix} P_0 \\ Q_0 \\ P_{C2} \\ P_{S2} \end{bmatrix} = \begin{bmatrix} u_d^p & u_q^p & u_d^n & u_q^n \\ u_q^p & -u_d^p & u_q^n & -u_d^n \\ u_q^n & -u_d^n & -u_q^p & u_d^p \\ u_d^n & u_q^n & u_d^p & u_q^p \end{bmatrix} \begin{bmatrix} i_d^p \\ i_q^p \\ i_d^n \\ i_d^n \end{bmatrix} \quad (12)$$

Solving this equation in terms of grid currents components we could get current references for DVCC controller.
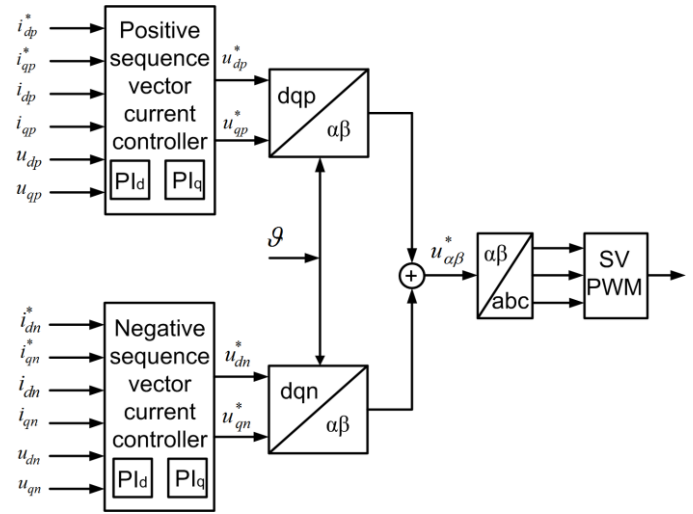

Figure 11. Dual vector current controller

Using this control structure, it is possible to eliminate DC link voltage oscillations, caused by unbalance, as well as oscillations in active power.

In order to protect power electronics converter currents in case of voltage sags are limited. As a consequence we will generate less power in case of disturbances, which will reflect on electrical torque of DG unit. Control of induction generator is classical indirect field vector control.

V. HIL EMULATION AND REAL-TIME IMPLEMENTATION

In this paper, a universal ultra-low latency HIL FPGA-based platform, dedicated to power electronics applications, is used [7]. The proposed platform comprises the emulator hardware and application software that supports a variety of circuit configurations. Electrical scheme which is emulated here is shown in Fig. 12. Power electronics hardware, which include generator, transformer, power part of power electronics converter and passive elements are emulated with the HIL600 platform with a time step of 1 μs. More details about HIL device can be found in [6]. The system parameters can be easily modified through the appropriate graphical user interface. Used concept is shown in Fig. 13 Control algorithms

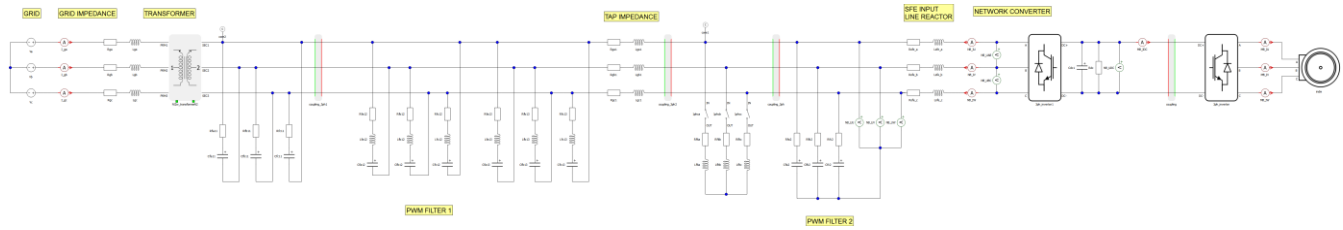are realized using a control platform based on TMS320F2812 DSP.

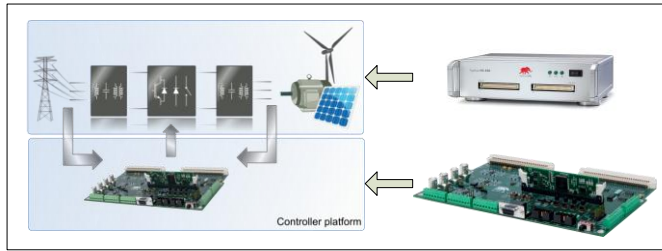Figure 12. Schematic diagram of DG system

Figure 13. HIL principle

VI. HIL EXPERIMENTAL RESULTS

In this section the performance of the proposed control principle is verified. Control algorithm is tested for three cases: performance in normal condition, behavior in case of balanced voltage sag and behavior in case of unbalanced voltage sag. Figs. 14 – 18 illustrate behavior of DG based system in normal voltage condition.
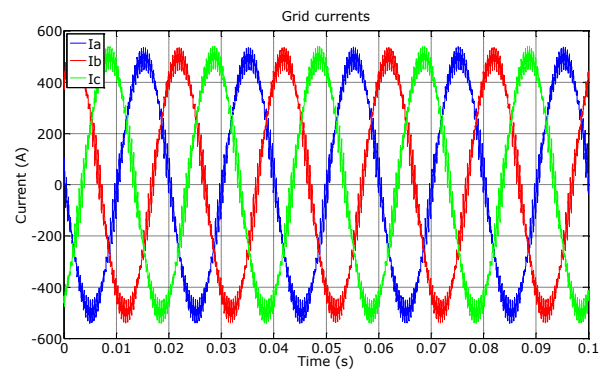

Figure 14. Grid voltages – no fault

Grid voltages are nominal with the line voltage of 400 V. Parameters of electrical transformer are: 1.5 MVA, 11.4/0.63 kV/kV. When we say voltage, we think of voltage after the transformer. From Fig. 15 we can see that grid currents are balanced. There is some ripple due to chosen switching frequency of 2 kHz, but PWM filter cut off most of it. It is the similar with the generator line currents, shown in Fig. 16. Machine electrical torque is quite constant and equals 2500 Nm. DC bus voltage is also stable, which indicate that the power transfer is correctly managed. In this case generator produce 560 kW of active power, while the reactive power is keep to zero.

Figure 15. Grid currents – no fault
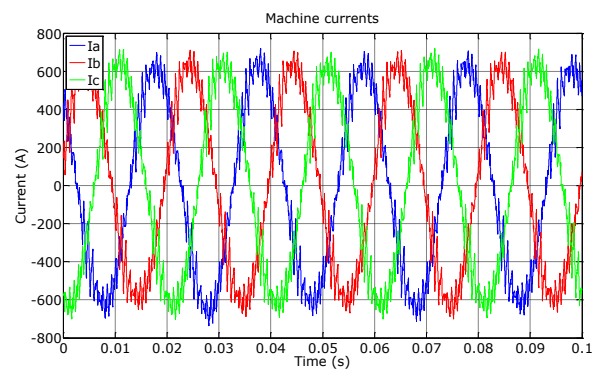
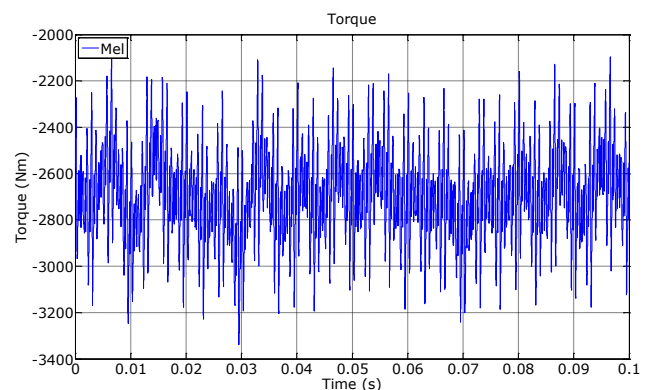Figure 16. Machine currents – no fault

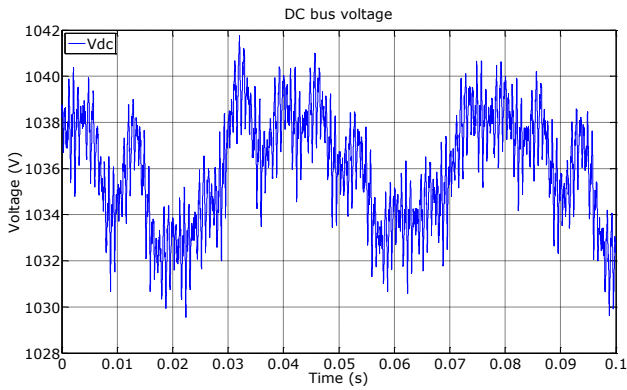Figure 17. Machine electrical torque – no fault

Figure 18. DC bus voltage – no fault

Figs. 19 – 23 show test results in case of balanced voltage sag. Balanced voltage sag is introduced using RL impedance and contactor. With the proper selection of R and L we can chose the depth of voltage sag.
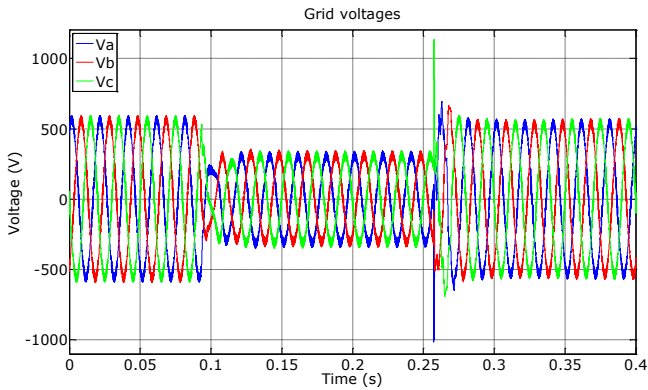

Figure 19. Grid voltages – Voltage sag type A

Fig. 19 shows grid voltage in case of balanced voltage sag to the 49% of the nominal voltage. We can see transient in the instant of voltage change which is due to RL circuit dynamic. During the voltage sag grid currents are higher than nominal, but they are limited in accordance to the grid side converter protection. A lower grid voltage and limited grid current imply a decrease in active power flow from the generator to the grid.
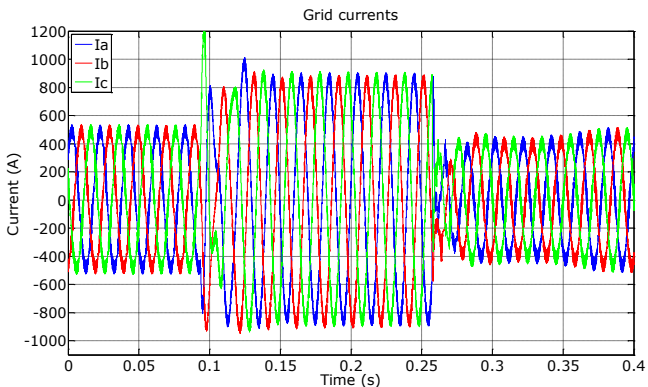

Figure 20. Grid currents – Voltage sag type A

In order to keep power flow balance it is necessary to reduce energy production of the distributed generator. This is achieved by proper reduction of torque reference. We can see in Fig. 22 that electrical torque during the voltage sag is reduced. In accordance with that generator currents are also reduced. DC bus voltage is still stable, except during transient, where we have a little deviation. DC bus stability is indicator that the power flow is correctly managed.
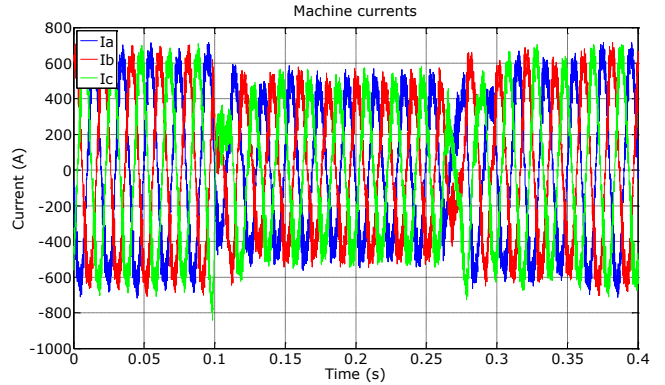

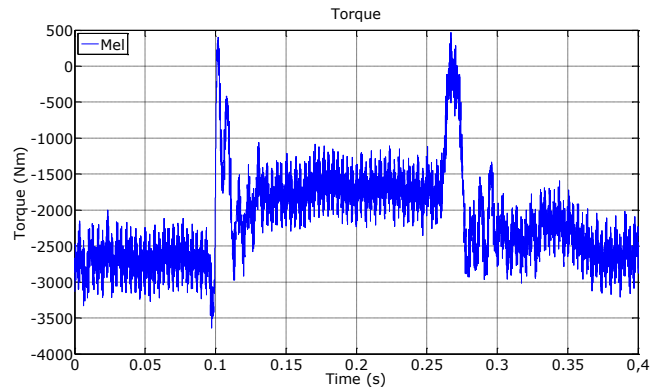Figure 21. Machhine currents – Voltage sag type A

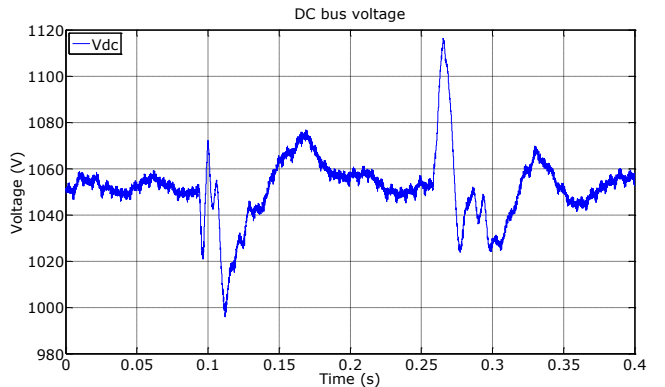
Figure 22. Electrical torque – Voltage sag type A

Figure 23. DC bus voltage – Voltage sag type A

The results shown in Fig. 24 – 28 show the response on unbalanced voltage sag type E. Two phases drop to 50 % of the nominal voltage, while third one stay the same as before the voltage sag. Before the voltage sag active power injected to the

grid was 300 kW. We can see that during the voltage sags currents are sinusoidal, but unbalanced. Currents are a little bit higher than the values before sags. Due to limited currents and lower grid voltages, power injected to grid is lower. This means that the production of the generator is a little bit lower, due to the fact that generator speed is kept constant. DC bus voltage is stable in this case, which means that our DVCC controller work properly.
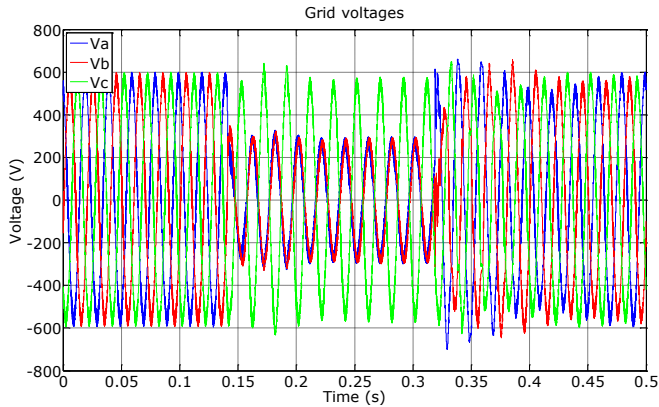

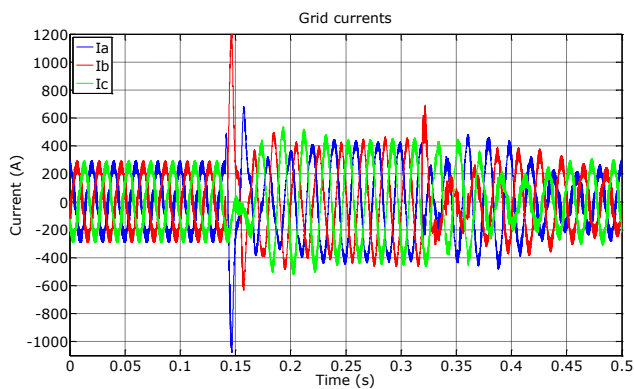Figure 24. Grid voltages – Voltage sag type E

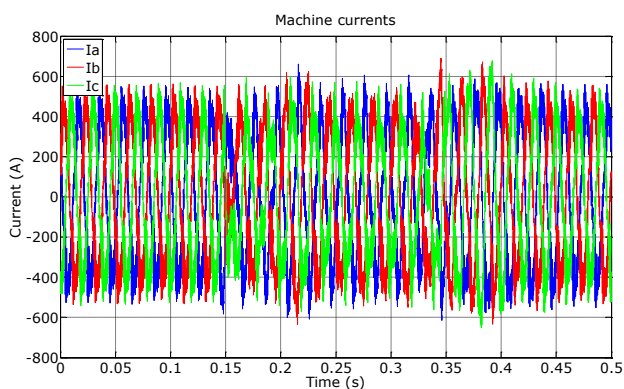Figure 25. Grid currents – Voltage sag type E

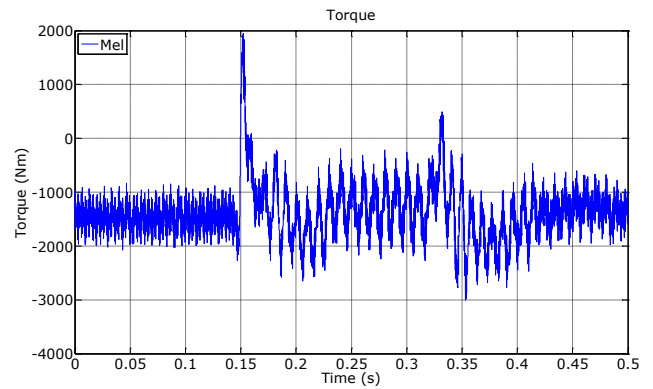Figure 26. Machine currents – Voltage sag type E

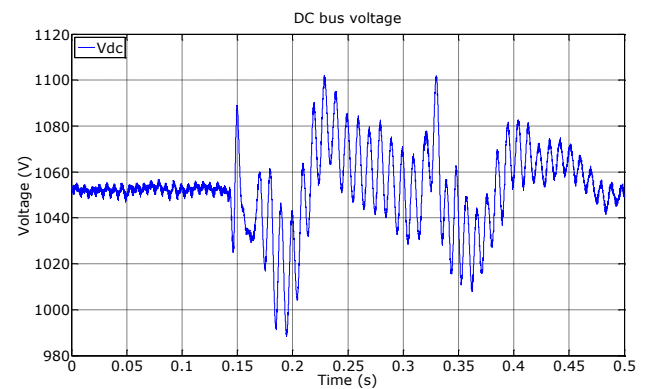Figure 27. Electrical torque – Voltage sag type E

Figure 28. DC bus voltage – Voltage sag type E

VII.   CONCLUSION

In this paper voltage ride-through behavior of distributed generator has been investigated. The performance of DVCC has been presented for balanced and unbalanced voltage sags. Proposed control algorithm enable distributed generator to stay connected to the grid during the disturbances and to inject active and reactive power in accordance with its capability. Algorithm principles are verified using Hardware-in-the-Loop emulation platform and TMS320F2812 DSP platform.

ACKNOWLEDGMENT (HEADING 5)

REFERENCES

[1]   M. Ezzat, M. Benbouzid, S.M. Muyeen and L. Harnefors, "Low-voltage ride-through techniques for DFIG-based wind turbines: state-of-the-art review and future trends," *In Proc. IEEE IECON 2013*, Viene Austria, November 2013, pp.236-242.

[2]   Y. Yang and F. Blaabjerg, "Low-voltage ride-through capability of a single-stage single-phase photovoltaic system connected to the low-

voltage grid," *International Journal of Photoenergy*, Article ID 257487, 2013.

[3] F. Hassan, "On power electronics interface for distributed generation applications and its impact on system reliability to customers," *Technical report,* Chalmers University of Technology, Sweeden 2005.

[4] F. Magueed, A. Sannino, "Design of robust converter interface for wind power applications," *Wind energy*, *published by Wiley Interscience*, vol. 8, pp. 319–332, Jul. 2005.

[5] Z. Ivanović, E. Adzić, M. Vekić, S. Grabić, N. Čelanović, V. Katić, "HIL evaluation of power flow control strategies for energy storage connected to smart grid under unbalanced conditions," *IEEE Trans. Power electron.*, USA, vol. 27, no. 11, pp. 4699–4710, Nov. 2012.

[6] N. Čelanović, I. Čelanović, Z. Ivanović, "Cyber Physical Systems: A new approach to power electronics simulation, control and testing, " *Advances in electrical and ųomputer engineering*, Faculty of electrical engineering and computer sciences, University of Suceava, Romania, issue 1, Feb. 2012, pp. 33–38.

[7] L. Zhang, M. Boolen, "Characteristic of voltage dips (sags) in power systems," *IEEE Trans. Power Del*., Vol. 15, No. 2, pp. 827 – 832, April 2000.

[8] F. Magueed, A. Sannino, J. Svensson, "Design of robust interface for wind power applications", *In Proc. Nordic Power Conference*, March 2004, pp. 1–6.

[9] S. Bifaretti, P. Zanchetta, A. Watson, L. Tarisciotti, J. C. Clare, "Advanced power electronic conversion and control system for universal and flexible power management," *IEEE Trans. Smart Grid*, vol. 2, issue 2, pp. 231–243, May 2011.

[10] T. Noguchi, H. Tomiki, S. Kondo, I. Takahashi, "Direct power control of PWM converter without power-source voltage sensors," *IEEE Trans. Ind. Appl*., Vol. 34, pp. 473 – 479, May/Jun. 1998.

[11] O. Bellmunt, A. Ferre, A. Sumper, J. Jane, "Ride-through control of a doubly fed induction generator under unbalanced voltage sags," *IEEE Trans. Energy Convers.*, vol. 23, no. 4, pp. 1036–1045, Dec. 2008.

[12] H. Song, K. Nam, "Dual current control scheme for PWM converter under unbalanced input voltage conditions," *IEEE Trans. Ind. Electron.*, vol. 46, no. 5, pp. 953–959, Oct. 1999.

[13] G. Saccomando, J. Svensson, A. Sannino, "Improving voltage disturbances rejection for variable-speed wind turbines," *IEEE Trans. Energy Convers.*, vol. 17, no. 3, pp. 422–428, Sept. 2002.

[14] Z. Ivanovic, M. Vekic, S. Grabic, V. Katic, "Control of multilevel converter driving variable speed wind turbine in case of grid disturbances," *in Proc. 12th IEEE EPE-PEMC*, Portoroz, Slovenia, Aug./Sept. 2006, pp. 1569–1573.

[15] C. Ng, L. Ran, "Unbalanced-grid-fault ride-through control for a wind turbine inverter," *IEEE Trans. Ind. Appl.*, vol. 44, no. 3, pp. 845–856, May/Jun. 2008.

[16] Y. Suh, Y. Go, D. Rho, "A comparative study on control algorithm for active front-end rectifier of large motor drives under unbalanced input," *IEEE Trans. Ind. Appl.*, vol. 47, no. 3, pp. 1419–1431, May/Jun. 2011.

[17] Y. Suh, T. Lipo, "Control scheme in hybrid synchronous stationary reference frame for PWM AC/DC converter under generalized unbalanced operating conditions," *IEEE Trans. Ind. Appl.*, vol. 42, no. 3, pp. 825–835, May/Jun. 2006.

[18] F. Wang, J. L. Duarte, M. Hendrix, "Pliant active and reactive power control for grid interactive converters under unbalanced voltage dips", *IEEE Trans. Power Electron.*, vol. 26, no. 5, pp. 1511–1521, May. 2011.

[19] R. K. Sinha, R. Kumar, M.Venmathi, L. Ramesh, " Analyses of voltage sags with different DG for various faulty conditions," *International Journal of computer communication and information system*, Vol. 12., No. 1, ISSN 0976 1349, Dec. 2010.

[20] M. Boolen, "Voltage recovery after unbalanced and balanced voltage dips in three-phase systems," *IEEE Trans. Power Del*., Vol. 18, No. 4, pp. 1376 – 1381, October 2003.